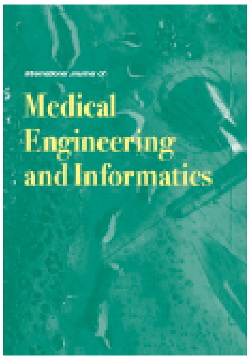

International Journal of Medical Engineering and Informatics

ISSN online: 1755-0661 - ISSN print: 1755-0653
https://www.inderscience.com/ijmei

Cloud and online system of 3D printing for serving multi-client of hospitals and medical colleges in different locations

Ignatius Luddy Indra Purnama, Alva Edy Tontowi, Herianto

DOI: 10.1504/IJMEI.2021.10043869

Article History:

Received:	16 June 2021
Accepted:	01 November 2021
Published online:	22 December 2023

Cloud and online system of 3D printing for serving multi-client of hospitals and medical colleges in different locations

Ignatius Luddy Indra Purnama,
Alva Edy Tontowi* and Herianto

Faculty of Engineering,
Gadjah Mada University,
Grafika Kampus Street,
Yogyakarta – 55281, Indonesia
Email: ignluddyindrap@ugm.ac.id
Email: alvaedytontowi@ugm.ac.id
Email: herianto@ugm.ac.id
*Corresponding author

Abstract: This manuscript presents a 3D printing method, especially human bone anatomy, in a cloud and online system. The human bone anatomy, specific skull and foot bone, of the patient's digital imaging and communications in medicine (DICOM) file, is uploaded to the so-called 3DPNet-DICOM cloud. After printing, the 3DPNet-DICOM cloud sends a notification and the 3D printed bone model to the hospital by courier. The 3D images constructed from the DICOM file and the 3D printed model was identifiable with no significant dimensional errors. The result is to eliminate the human operators' activity, and queuing at the order process.

Keywords: 3D printing; bone model; cloud application; online application; DICOM; network access.

Reference to this paper should be made as follows: Purnama, I.L.I., Tontowi, A.E. and Herianto (2024) 'Cloud and online system of 3D printing for serving multi-client of hospitals and medical colleges in different locations', *Int. J. Medical Engineering and Informatics*, Vol. 16, No. 1, pp.23–33.

Biographical notes: Ignatius Luddy Indra Purnama is a Doctoral student in Industrial Engineering at the Gadjah Mada University, Yogyakarta, Indonesia. He received his Master's in Manufacturing System Engineering at the Asian Institute of Technology, Bangkok, Thailand. His current focus of research is on management technology and information, and production systems.

Alva Edy Tontowi is a Professor in Industrial Engineering at the Department of Mechanical and Industrial Engineering, Faculty of Engineering, Gadjah Mada University, Yogyakarta, Indonesia. He received his PhD from the Leeds University, UK. His research interests are biomedical engineering, manufacturing engineering, and the 3D printing process.

Herianto is an Associate Professor in Industrial Engineering at the Department of Mechanical and Industrial Engineering, Faculty of Engineering, Gadjah Mada University, Yogyakarta, Indonesia. He received his PhD from the Tokyo Institute of Technology, Japan. His research interests are mechanical and control engineering and the 3D printing process.

1 Introduction

A computer tomography (CT) can acquire anatomic images of specific areas of interest, such as human bone anatomy. A CT scan is easily made available and is the preferred imaging technique for studying bone structures. When CT scan results are available, the doctor can explain the results to the patient. Patients may difficult to understand the doctor's explanation of the X-ray image (Bücking et al., 2017; McCabe and Healey, 2018), and may not thoroughly interpret the X-ray images after clarification by the doctor (Scholz et al., 2019). Patients might better understand their condition if presented with a 3D physical model rather than an X-ray image (Zheng et al., 2018). At present, the entire 3D printing process is manually performed by human operators (Osti et al., 2019). The manual 3D printing process in hospitals and its application software tools are burdened by the standard processing time, need for operators, and order queues of the 3D printing process (Ramola et al., 2019).

In biomedical applications, low-cost 3D-Printing is becoming more popular as it offers an opportunity to personalise patient care (Aimar et al., 2019). In addition to the use of 3D printed models to assist patient consultation with doctors, it is also used to build and install customised surgical devices and organs, clinical practice and training models, clinical testing models, tissue engineering, drug delivery, bone-implant replacement, and operation planning using the 3D printers in biomedical (Ahangar et al., 2019; Bose et al., 2018). A cloud and online system of 3D printing service would support any hospitals and medical colleges in a different location.

Digital 3D printed models are also expected to become extensively used at a low cost in biomedical fields (Carbonaro et al., 2020). 3D printing processes in the cloud are the future direction of 3D printing research (Navale and Bourne, 2018). Infrastructure as a framework and platform as a service has developed medical imaging with rendering methods through cloud computing technology, but the disadvantage is that the images are not online or interactive. (Bücking et al., 2017). Communication between the cloud and the 3D printer remains an offline service in biomedicine (Zhang et al., 2019)

This study proposes a new printing method called 3DPNet-DICOM cloud. Combining a 3D printer, a point cloud, and an online system, this method prints a human bone anatomical part directly from the DICOM file. The model 3D printed can help patients understand the doctor's explanation. The expected clients of 3DPNet-DICOM are CT scan operators and doctors in hospitals and medical colleges. We will highlight how 3DPNet-DICOM can serving multi-client of hospitals and medical colleges in different locations. In an evaluation study, the 3D images were constructed from the DICOM file and the 3D printed model, to eliminate the human operators' activity, and queuing at the order process.

The following is the outline for the paper. Section 2 reviews relevant literature about cloud, online and 3D printer applications in biomedical. Section 3 research methods include the current framework, design of the proposed framework and experiment tools. Section 4 discusses the result. Finally, Section 5 concludes the study and provides contributions as well as future research directions.

2 Literature review

3D printing technology is used to create human organs from exact CT scan scans (Radenkovic et al., 2016). 3D printers can be a cost-effective, on-demand method of fabricating complex geometric items in practically any shape with various materials, including metals, polymers, ceramics, and bioinks (Ahangar et al., 2019). 3D printer technology for biomedical (Walker, 2017), healthcare (Dodziuk, 2016), and radiologist (Mitsouras et al., 2015) applications in both research and clinical settings (Aroca et al., 2017). Low-cost 3D printed models can transform various medical picture modalities, which is helpful for better understanding the geometric structure and complex spatial features of anatomical organs (Shui et al., 2017). When paired with medical imaging, 3D printing creates a powerful combination that has substantially impacted medicine. It is utilised to construct unique prosthetics, teach trainees how to conduct complex procedures, and develop anatomical models to aid complex operations (Marro et al., 2016). 3D printers that use fused deposition modelling (FDM) have recently become popular in the industrial and medical areas. The nozzle temperature setting can be automatically adjusted by a cyber physics system (CPS), considerably minimising the distortion of 3D printed models (Miao et al., 2019). There are three steps from medical photos to 3D printed models: picture segmentation, mesh refining, and 3D printing (Bücking et al., 2017).

Bone printing using a 3D printer is beneficial in facilitating medical education, primarily helping introduce bone structure, bone tissue, and temporal bone as tools for otologic. Because using cadaver bones is related to ethics (Gadaleta et al., 2020; Hann et al., 2021). Furthermore, the utilisation of 3D printing techniques to generate one-of-a-kind specific structures that can reconstruct or remodel certain structures in human bones (Bose et al., 2018). Image processing technologies and segmentation techniques can be used to analyse the bone structure to create a solid model for 3D printing (Cho et al., 2015). The segmentation procedure can perfectly build a prototype temporal bone model by quick 3D printing of CT scans with clinical quality (Cohen and Reyes, 2015). A handmade medical 3D printer with a printing resolution of 0.1 mm can also be used for bespoke bone printing (Yoon et al., 2016). All the 3D printing techniques are currently unavailable. In manufacturing, 3D printers and cloud production usage has shown considerable potential (Guo and Qiu, 2018; Zhang et al., 2020). 3D printing services are being developed to minimise manufacturing time, costs and increase service quality. Multi-task scheduling in 3D printing services is one solution dispersed in cloud manufacturing (Liu et al., 2021). Cloud-based 3D printing services are also being developed for small and medium-sized businesses (Chu et al., 2018). Future access protocols on the manufacturing cloud platform can use an application programming interface (API) and a remote monitoring system (Baumann et al., 2017; Yiming et al., 2017).

The 3D printing model was validated by measuring the anterior-posterior (A-P), left-right (L-R), and top-bottom (T-B) length differences between the 3D image and the 3D printed model. The size of the 3D image model was calculated using InVesalius software, and the dimensions of the 3D printed model were measured by the calliper method. The A-P and L-R lengths were measured from the axial slices, the T-B and A-P lengths were measured from the sagittal slices, and the L-R and T-B lengths were measured from the coronal slices. The A-P, L-R, and T-B dimensions were then calculated by equations (1), (2), and (3), respectively. All measurements were taken by four observers (Odeh et al., 2019).

$$\text{A-P} = \max(\text{A-P length in axial slice, A-P length in sagittal slice}) \tag{1}$$

$$\text{L-R} = \max(\text{L-R length in axial slice, L-R length in coronal slice}) \tag{2}$$

$$\text{T-B} = \max(\text{T-B length in sagittal slice, T-B length in coronal slice}) \tag{3}$$

3 Research method

In the current condition, some hospitals and medical schools are producing 3D printed models in-house. However, if the hospitals and medical schools cannot fulfil all 3D printing orders, the 3D printing is outsourced to an external production unit. Transfer data in the 3D printing process in-house, in hospitals and medical colleges, are using an SD Card with a human courier or USB type-B cable. But for the external, transfer data in the 3D printing process between hospitals and medical schools with external 3D printing process units are using an email. Manual printing from a DICOM format file to a 3D printed model involves three processes. In the first step, the bone segment is reconstructed using software such as InVesalius, LeadTools, MevisLab, or Embodi3D. The second step is setting the 3D printer parameters, and resizing, slicing, and generating the G-Code command using software such as Slic3r, Replicator G, Cura, FreeCAD, or All3DP. The G-Code format file is transferred to the 3D printer. Finally, the G-Code command is executed on the 3D printer using Marlin Firmware software. At some hospitals, medical colleges, and external production units, each step of the process is performed by a single human or separate human operator for all processing steps.

In the present study, a bone object is printed using the 3DPNet-DICOM cloud. The 3DPNet-DICOM cloud is accessible to hospital staff, especially the CT scan operator as a customer. Customers can upload 3D images from a CT scan to the 3DPNet-DICOM cloud as a DICOM file through the VPN platform with an HTTPS protocol for security. The 3DPNet-DICOM cloud converts the DICOM file to stereolithography (STL) format. If the 3D printer is idle, the STL file is translated into a G-Code file and delivered to the 3D printer via a WiFi router and Raspberry Pi 3. When the 3D printer has finished running, 3DPNet-DICOM notifies the customer by email.

The 3DPNet-DICOM cloud is encoded in Python 3 and runs on the operating system Linux (Ubuntu 18). Python and Linux were selected because they are open-source and free of charge. 3DPNet-DICOM source code can access via permanent connection https://github.com/luddy-indra/3DPNet-DICOM. The license under the legal law is GNU General Public License v.3. The 3DPNet-DICOM software runs in two main stages. The first stage converts a DICOM file into an STL file. Two modules – the initialisation module and the STL-convert module operate in a flask environment. The initialisation module performs the registration and login of the customer, displays the customer's profile, and uploads a DICOM file in zip file format. Customer data will be saved in the customer database, and a zip file will be saved in the history_zip and temporary_zip folders. The STL-convert module converts a DICOM file into the STL file module. Its functions perform extraction from the zip file, loading of the 3D image file, bone segmentation, and saving the bone segmentation in the STL file. STL file will be saved in the history_stl and temporary_stl folders. The second stage converts the STL file into a G-Code file and delivers it to the 3D printers. The functions of the second stage check the 3D printer status, resize the 3D image dimensions to those of the working area of the 3D printer, slice the 3D image, generate a G-Code file, deliver the G-Code file to the 3D printer, delete the G-Code file from upload folder after printing, and send an email notification to the customer.

The mesh 3D image reconstruction is performed by improved marching cube algorithm (IMCA), the algorithm is relatively simple (Masala et al., 2013). The threshold of IMCA is 200 for a single-slice CT scan (Purnama et al., 2019), and 210 for a multi-slice CT scan (Purnama et al., 2020b). The algorithm that resizes the 3D image dimensions reduces the 3D image size by 5% decrements until the 3D image size is equal to or less than the working area of the 3D printer.

3D image slicing and generate G-Code process through an application program interface (API) with CuraEngine ver. 15.04.6. The API software sets the parameters of the 3D printer, performs the slicing, and generates the G-Code commands following the 3D printer's specifications (Baumann et al., 2017; Purnama et al., 2020a). So, 3DPNet-DICOM software can access only 3D printers that are compatible with CuraEngine software. The 3D printer parameters are the nozzle temperature and size, the support material and its specifications, and the speed, fill density, machine setting, and printer-head size of the printer.

The experimental data were sampled from DICOM files of a skull and a foot bone extracted from the DICOM library (sourced from https://www.dicomlibrary.com/). The 3D images of the skull and foot bone were constructed from 181 and 192 slices, respectively. All skull and foot bone slices have the same dimensions (512 mm × 512 mm). The experiment was performed on a low-cost fused deposition modelling (FDM) 3D printer, with specification: the x-y-z dimensions of the 3D printer were 110 mm × 120 mm × 170 mm, the gantry height and nozzle size were 55 mm and 0.4 mm, respectively, the compatible material diameter was 1.75 mm, and the printing temperature and speed were 200°C and 60 mm/s, respectively. The travel speed was 120 mm/s, and no heated bed was required. The material was filament polylactide (PLA) with a diameter of 1.75 mm. The 3D printing model was validated by measuring the A-P, L-R and T-B length differences between the 3D image and the 3D printed model. The researcher determines the A-P, L-R, and T-B point that has the widest area. The size of the 3D image model was calculated using InVesalius software, and the dimensions of the 3D printed model were measured by the calliper method. A-P, L-R, and T-B measurements were carried out by four observers.

4 Result and discussion

4.1 3DPNet-DICOM cloud queue

Customers can access the 3DPNet-DICOM software from a computer, laptop, tablet, or smartphone connected to the Internet. The login process protects the privacy and data of the consumer. Stage 1 of the 3DPNet-DICOM flowchart can be simultaneously processed for multiple customers, negating the need for queuing. In the 3DNet-DICOM cloud, customers are queued only in stage 2 (which involves resizing, slicing, and creating a G-Code process), because this stage proceeds only when a 3D printer is available. So it is potentially a bottleneck at stage 2.

4.2 Total processing times of manual 3D printing and 3DPNet-DICOM cloud

Table 1 compares the standard processing times of 3DPNet-DICOM cloud and manual 3D printing with application software tools. 3DPNet-DICOM cloud reduced the standard processing time by approximately 90% in stage 1, and by 80% in stage 2a. In stage 2b, the times of processing the skull and foot bone by the manual and 3DPNet-DICOM cloud methods were decreased by 6–10%, respectively.

Table 1 Comparison of standard processing time for existing and 3DPNet-DICOM cloud

Stage	*Activity*	*Standard processing time*			
		Existing		*3DPNet-DICOM*	
		Skull	*Foot-bone*	*Skull*	*Foot-bone*
1	3D image reconstruction and bone segmentation process	5 minutes	4 minutes	30.45 seconds	23.50 seconds
2a	Resizing, slicing, and generate G-Code process	2.5 minutes	2 minutes	25.05 seconds	20.10 seconds
2b	Setup and 3D-Printingprocess	16 hours	5 hours	15 hours	hours

The work performed by human operators was considerably reduced by the 3DPNet-DICOM cloud. Users of the 3DPNet-DICOM cloud only to the segmentation process (in stage 1) and the resizing process (in stage 2a). As segmentation and resizing require high concentration and accuracy, both processes can quickly tire the operator. Moreover, the allowance factors of close attention are very exacting, the mental strain is complex, and the monotony and tediousness factors are high. Elimination of human operators in stages 1 and 2a would reduce the operational costs. After production, cleaning the 3D printed model from its support is difficult because PLA is a weak material. Cleaning the 3D-printed model thus requires patience, caution, accuracy, and time. The 3DPNet-DICOM cloud requires an operator to remove the 3D printed model from the 3D printer workbench and clean its support.

4.3 3D-printed model by 3DPNet-DICOM cloud

Under the specifications of the FDM 3D printer, the 3D printed models of the skull and foot bone were scaled by 40% and 30%, respectively. The extruded layers, total print times, filament lengths, and weights of the 3D printed models were 262, 15.0 hours, 35.21 m, and 25 g for the skull, and 257, 4.5 hours, 7.88 m, and 15 g for the foot bone. The 3D printed models of the skull and foot bone are displayed in Figures 1 and 2, respectively. Both models are presented from the axial, sagittal, and coronal sides. The actual dimension of the 3D printed skull model is 85 mm × 62.8 mm × 101 mm and 3D printed foot bone model is 88.3 mm × 61 mm × 43 mm.

Figure 1 3D printing model of the skull from the (a) axial side, (b) sagittal side and (c) coronal side (see online version for colours)

(a) (b) (c)

Figure 2 3D printing model of the foot bone from the (a) axial side, (b) sagittal side and (c) coronal side (see online version for colours)

(a) (b) (c)

4.4 Validation of 3D printing model

Table 2 lists the physical measurements of the 3D images and 3D printed models of the skull and foot bone. The A-P, L-R and T-B features of both models were calculated by equations (1), (2), and (3), respectively. In the validation process, the 3D printed model skull and foot bone measurements of 40% and 30%, respectively, were equalised to 100%. All measurements of the 3D images and 3D printed models differed by less than 0.001 mm. It was concluded that the 3D image and the 3D-printed model were identifiable with no significant dimensional error.

Table 2 Physical measurement of 3D image model and 3D-printing model

Object sample	*Feature*	*3D image model measurement/3D-printing model measurement in mm (% difference)*				*± Standard deviation action 4 observers*		
		Observer 1	*Observer 2*	*Observer 3*	*Observer 4*	*3D image model (mm)*	*3D-printing model (mm)*	*% difference*
Skull	A-P	212.501/212.500 (100.0005)	212.503/212.500 (100.0014)	212.502/212.500 (100,0009)	212.502/212.500 (100.0009)	0.0008	0.0000	0.00038
	L-R	157.001/157.000 (100.0006)	157.003/157.000 (100.0019)	157.002/157.000 (100.0013)	157.003/157.000 (100.0019)	0.0010	0.0000	0.00061
	T-B	252.501/252.500 (100.0004)	252.502/202.500 (100.0008)	252.504/252.500 (100.0016)	252.502/202.500 (100.0008)	0.0005	0.0000	0.00050
Foot bone	A-P	294.334/294.300 (100.0116)	294.335/294.300 (100.0119)	294.334/294.300 (100.0116)	294.334/294.300 (100.0116)	0.0005	0.0000	0.00017
	L-R	203.334/203.300 (100.0167)	203.335/203.300 (100.0172)	203.334/203.300 (100.0167)	203.334/203.300 (100.0167)	0.0005	0.0000	0.00025
	T-B	143.334/143.300 (100.023)	143.335/143.300 (100.0244)	143.336/143.300 (100.0251)	143.334/143.300 (100.0237)	0.0010	0.0000	0.00067

Note: A-P – anterior and posterior; L-R – left and right; T-B – top and bottom.

5 Conclusions

The 3DPNet-DICOM cloud is an open-source application, especially for human bone anatomy, that runs well in the Linux (Ubuntu 18) operating system. The intended customers of this software are doctors and CT-scan operators in hospitals and medical colleges in different locations. The software inputs a DICOM file (a 3D image from a CT scanner) in zip file format and outputs a 3D printed model of bone structures. 3DPNet-DICOM reduced the standard processing time of 3D-image on stages 1 and 2a by reducing the human operator activity. In stage 2b, it was decreased by reducing material support. Queues at the beginning of the process were removed because stage 1 of the 3DPNet-DICOM flowchart can simultaneously process multiple customers. The 3D images from DICOM and the 3D printing models were identifiable with significant dimensional errors. The model 3D printed can help patients understand the doctor's explanation.

In future research, the 3DPNet-DICOM cloud data will be validated on another 3D printer with different materials (rigid, semirigid, and flexible materials) (Garcia et al., 2018). Furthermore, the position of the 3D image in the work area of the 3D printer will be optimised to reduce the material support of the 3D printed model.

References

Ahangar, P., Cooke, M.E., Weber, M.H. and Rosenzweig, D.H. (2019) 'Current biomedical applications of 3D printing and additive manufacturing', *Applied Sciences*, Vol. 9, No. 8, p.1713.

Aimar, A., Palermo, A. and Innocenti, B. (2019) 'The role of 3D printing in medical applications: a state of the art', *Journal of Healthcare Engineering*, Vol. 2019, No. 95, pp.1–10.

Aroca, R.V., Ventura, C.E.H., De Mello, I. and Pazelli, T.F.P.A.T. (2017) 'Sequential additive manufacturing: automatic manipulation of 3D printed parts', *Rapid Prototyping Journal*, Vol. 23, No. 4, pp.653–659.

Baumann, F.W., Kopp, O. and Roller, D. (2017) 'Abstract API for 3D printing hardware and software resources', *The International Journal of Advanced Manufacturing Technology*, Vol. 92, No. 1–4, pp.1519–1535.

Bose, S., Robertson, S. and Bandyopadhyay, A. (2018) '3D printing of bone implants and replacements', *American Scientist*, Vol. 106, No. 2, p.112.

Bücking, T.M., Hill, E.R., Robertson, J.L., Maneas, E., Plumb, A.A. and Nikitichev, D.I. (2017) 'From medical imaging data to 3D printed anatomical models', in Chen, H-C.I. (Ed.): *PLOS ONE*, Vol. 12, No. 5, p.e0178540.

Carbonaro, D., Putame, G., Castaldo, C., Meglio, F. Di, Siciliano, K., Belviso, I., Romano, V. et al. (2020) 'A low-cost scalable 3D-printed sample-holder for agitation-based decellularization of biological tissues', *Medical Engineering and Physics*, Vol. 85, No. 3, pp.7–15, Elsevier Ltd.

Cho, J., Park, C-S., Kim, Y-J. and Kim, K.G. (2015) 'Clinical application of solid model based on trabecular tibia bone CT images created by 3D printer', *Healthcare Informatics Research*, Vol. 21, No. 3, p.201.

Chu, J., Gong, J., Yu, S. and Chen, J. (2018) 'Analysis and research on the application status of 3D Printing cloud service platform', *2018 10th International Conference on Intelligent Human-Machine Systems and Cybernetics (IHMSC)*, IEEE, Vol. 1, pp.239–242.

Cohen, J. and Reyes, S.A. (2015) 'Creation of a 3D printed temporal bone model from clinical CT data', *American Journal of Otolaryngology*, Vol. 36, No. 5, pp.619–624, Elsevier Inc.

Dodziuk, H. (2016) 'Applications of 3D printing in healthcare', *Polish Journal of Cardio-Thoracic Surgery*, Vol. 3, No. 3, pp.283–293.

Gadaleta, D.J., Huang, D., Rankin, N., Hsue, V., Sakkal, M., Bovenzi, C., Huntley, C.T. et al. (2020) '3D printed temporal bone as a tool for otologic surgery simulation', *American Journal of Otolaryngology*, Vol. 41, No. 3, p.102273, Elsevier Inc.

Garcia, J., Yang, Z.L., Mongrain, R., Leask, R.L. and Lachapelle, K. (2018) '3D printing materials and their use in medical education: A review of current technology and trends for the future', *BMJ Simulation and Technology Enhanced Learning*, Vol. 4, No. 1, pp.27–40.

Guo, L. and Qiu, J. (2018) 'Combination of cloud manufacturing and 3D printing: research progress and prospect', *The International Journal of Advanced Manufacturing Technology*, Vol. 96, Nos. 5–8, pp.1929–1942.

Hann, S.Y., Cui, H., Esworthy, T., Zhou, X., Lee, S. jun, Plesniak, M.W. and Zhang, L.G. (2021) 'Dual 3D printing for vascularized bone tissue regeneration', *Acta Biomaterialia*, Vol. 123, No. 18, pp.263–274, Elsevier Ltd.

Liu, S., Zhang, L., Zhang, W. and Shen, W. (2021) 'Game theory based multi-task scheduling of decentralized 3D printing services in cloud manufacturing', *Neurocomputing*, Vol. 446, No. 7, pp.74–85, Elsevier B.V.

Marro, A., Bandukwala, T. and Mak, W. (2016) 'Three-dimensional printing and medical imaging: a review of the methods and applications', *Current Problems in Diagnostic Radiology*, Vol. 45, No. 1, pp.2–9, Elsevier.

Masala, G.L., Golosio, B. and Oliva, P. (2013) 'An improved marching cube algorithm for 3D data segmentation', *Computer Physics Communications*, Vol. 184, No. 3, pp.777–782, Elsevier B.V.

McCabe, R. and Healey, P.G.T. (2018) 'Miscommunication in doctor-patient communication', *Topics in Cognitive Science*, Vol. 10, No. 2, pp.409–424.

Miao, G., Hsieh, S-J., Segura, J.A. and Wang, J-C. (2019) 'Cyber-physical system for thermal stress prevention in 3D printing process', *The International Journal of Advanced Manufacturing Technology*, Vol. 100, Nos. 1–4, pp.553–567.

Mitsouras, D., Liacouras, P., Imanzadeh, A., Giannopoulos, A.A., Cai, T., Kumamaru, K.K., George, E. et al. (2015) 'Medical 3D printing for the radiologist', *RadioGraphics*, Vol. 35, No. 7, pp.1965–1988.

Navale, V. and Bourne, P.E. (2018) 'Cloud computing applications for biomedical science: a perspective', in Ouellette, F. (Ed.): *PLOS Computational Biology*, Vol. 14, No. 6, p.e1006144.

Odeh, M., Levin, D., Inziello, J., Lobo Fenoglietto, F., Mathur, M., Hermsen, J., Stubbs, J. et al. (2019) 'Methods for verification of 3D printed anatomic model accuracy using cardiac models as an example', *3D Printing in Medicine*, Vol. 5, No. 1, pp.1–12.

Osti, F., Santi, G., Neri, M., Liverani, A., Frizziero, L., Stilli, S., Maredi, E. et al. (2019) 'CT conversion workflow for intraoperative usage of bony models: from DICOM Data to 3D printed models', *Applied Sciences*, Vol. 9, No. 4, p.708.

Purnama, I.L.I., Tontowi, A.E. and Herianto (2020a) 'Threshold determination in multislice CT-scan using improved marching cube algorithm (IMCA) for 3D image reconstruction process (3D-IRP)', *Journal of Physics: Conference Series*, Vol. 1655, p.012088, Riau.

Purnama, I.L.I., Tontowi, A.E. and Herianto (2020b) 'G-Code generator from bone DICOM CT with cloud', *Journal of Physics: Conference Series*, Vol. 1477, No. 6, p.062017.

Purnama, I.L.I., Tontowi, A.E. and Herianto (2019) '3D image reconstruction with single-slice CT using improved marching cube algorithm', *2019 International Biomedical Instrumentation and Technology Conference (IBITeC)*, IEEE, pp.84–87.

Radenkovic, D., Solouk, A. and Seifalian, A. (2016) 'Personalized development of human organs using 3D printing technology', *Medical Hypotheses*, December, Vol. 87, pp.30–33, Elsevier Ltd.

Ramola, M., Yadav, V. and Jain, R. (2019) 'On the adoption of additive manufacturing in healthcare: a literature review', *Journal of Manufacturing Technology Management*, Vol. 30, No. 1, pp.48–69.

Scholz, V., Lange, S., Rosenberg, B., Kromrey, M.-L., Syperek, A., Hosten, N., Kohlmann, T. et al. (2019) 'Identifying communication-related predictors of patient satisfaction in a briefing prior to contrast-enhanced computed tomography', *Insights into Imaging*, Vol. 10, No. 1, p.99.

Shui, W., Zhou, M., Chen, S., Pan, Z., Deng, Q., Yao, Y., Pan, H. et al. (2017) 'The production of digital and printed resources from multiple modalities using visualization and three-dimensional printing techniques', *International Journal of Computer Assisted Radiology and Surgery*, Vol. 12, No. 1, pp.13–23.

Walker, V. (2017) 'Implementing a 3D printing service in a biomedical library', *Journal of the Medical Library Association*, Vol. 105, No. 1, pp.55–60.

Yiming, G., Rong, Z., Zhisheng, Z. and Zhen, C. (2017) 'Design of remote monitoring system for 3D printing based on cloud platform', *2017 24th International Conference on Mechatronics and Machine Vision in Practice (M2VIP)*, IEEE, pp.1–5.

Yoon, D-K., Jung, J-Y., Shin, H-B., Kim, M-S., Choe, B-Y., Kim, S., Suh, T.S. et al. (2016) 'Fabrication of a customized bone scaffold using a homemade medical 3D printer for comminuted fractures', *Journal of the Korean Physical Society*, Vol. 69, No. 5, pp.852–857.

Zhang, C., Sheng, B., Yin, X., Zhao, F. and Shu, Y. (2019) 'Research and development of off-line services for the 3D automatic printing machine based on cloud manufacturing', *Journal of Ambient Intelligence and Humanized Computing*, Vol. 10, No. 3, pp.1109–1128, Springer Berlin Heidelberg.

Zhang, L., Luo, X., Ren, L., Mai, J., Pan, F., Zhao, Z. and Li, B. (2020) 'Cloud based 3D printing service platform for personalized manufacturing', *Science China Information Sciences*, Vol. 63, No. 2, p.124201.

Zheng, W., Chen, C., Zhang, C., Tao, Z. and Cai, L. (2018) 'The feasibility of 3D printing technology on the treatment of pilon fracture and its effect on doctor-patient communication', *BioMed Research International*, Vol. 2018, No. 121, pp.1–10.